MM Science Journal | www.mmscience.eu
ISSN 1803-1269 (Print) | ISSN 1805-0476 (On-line)
Special Issue | ICTIMT2021
2nd International Conference on Thermal Issues in Machine Tools
April 20, 2021, Prague, Czech Republic
DOI: 10.17973/MMSJ.2021_07_2021065

ICTIMT2021-029

COMPARISON OF METHODS FOR CONTROLLED THERMAL DEFORMATIONS IN MACHINE TOOLS

A. P. Kuznetsov [1]*, H. J. Koriath [2]

[1] Moscow State University of Technology STANKIN in Moscow, Department of Machine Tools, Moscow, Russia

[2] Fraunhofer Institute for Machine Tools and Forming Technology IWU, Automation and Monitoring, Chemnitz, Germany

*Corresponding author; e-mail: apk_53@mail.ru

Abstract
Progress in improving the accuracy of metal-cutting machines is inextricably linked and driven by deeper knowledge gained through the study of thermal processes and effects occurring in machines, which can be used to manage them. This led to the dominance of temperature errors in the balance of machine accuracy, the share of which changed from 20-30% to 70% during the period from 1950 to 2020, which is determined by the absolute value of the achievable machine accuracy. Types and forms of compensation methods were formed (1990-2020), which were based on the use of linear and nonlinear regression or correlation methods. Performing experiments can establish the functional relationship between the measured temperature in the machine nodes and the amount of displacement. With good repeatability and stable reproducibility of the result, an equation expresses this functional relationship. Applying this equation to a program, a control device compensates the thermal deformations. However, in all cases, it is necessary to determine the number and location of temperature measurements on the machine, determining the compensation accuracy. The proposed sensorless model is based on a thermal behavior model and does not require temperature measurements. A method is presented and justified for estimating the number of temperature measurement locations based on thermophysical analysis by applying the finite element method in comparison with the analytical method in order to achieve the required compensation accuracy. For several machine tool types, a comparison is given regarding the control method of the TCP spindle displacement without sensors and with temperature sensors. The limits of their rational use are presented.

Keywords:
machine tool; temperature processes and effects; control; compensation; sensors

1 INTRODUCTION

The high requirements on the accuracy parameters of the products processed on the machine tools make it necessary to constantly increase the accuracy of the machine tools and to create systems and methods of control, ensuring the output parameters of machine tool accuracy.

From 1980 to 2000, a progress was enabled in the development of methods: analysis of the types of elementary error components, a variation method of calculating the accuracy of machines, geometric representation of homogeneous transformations of coordinate systems, the motion accuracy (formation of shapes) based on homogeneous transformations of coordinate systems, kinematics of quasi solid rigid bodies.

Between 2000 and 2020, new methods of describing accuracy have appeared, including: volumetric errors of non-solids; three-dimensional errors of solids and non-solids; the theory of the kinematics of multi-systems (MBS); geometric accuracy, shape and surface characteristics of machine tools using state field functions; models based on Denavit-Hartenberg (D-H) designations; models of geometric errors in machine tools using the exponent product formula (PoE) and models based on the PoE screw theory.

Thus, it is possible to systematize research directions on the control of thermal processes and effects in machine tools [Yto 2010], [Mayr 2012] as follows: reduction of the number of heating sources; heat flow control; design of a heat-resistant machine structure; correction or compensation of thermal errors; process control of numerical compensation of errors (which depend exclusively on temperature or depend both on the condition and temperature of machine parts).

The following types and forms of compensation methods originated between 1990 and 2020, which were based on [Mayr 2012], [Blaser 2019], [Kuznetsov 2018], [Xian 2018],

[Kuznetsov 2015]: direct methods of measured temperature errors; indirect methods on the measured temperature that is obtained from sensors (or without sensors) located at different points of the machine and from the subsequent determination of the TCP offsets on the thermal model; indirect methods on the information obtained from sensors or without sensors, on various parameters (such as speed, speed of movement on the axes, etc.) and calculation on the basis of the constructed or selected mathematical model; program methods on the basis of thermophysical or thermoelastic machine tool model; predicted models of changes in temperature deformation; methods of training the machine control system based on experimental data of thermal machine tool behavior; combined with other methods, including combinations of the previous ones.

2 CONTROLLED THERMAL DEFORMATIONS

Consequently, the only common link in all these methods is the model (thermophysical or mathematical), whose degree of detail depends on the choice of a particular control method, which is especially important when using predictive software sensor systems or sensorless systems. These systems, depending on the required accuracy of control, require the justification of both the location of sensors and their number, and the regularities of change (behavior) of the final control, such as the machine's TCP. For example, analyzing a number of studies has shown that the number of temperature sensors is offered from 2 to 76 [Abdulshahed 2015], [Hui 2020], [Chen 2016] or a sufficient or necessary number [Naumann 2018] without justifying either (the number) or the other (the location on the machine part). Therefore, the purpose of this study is to justify these characteristics for a typical machine temperature model.

2.1 Thermoelastic structure

It is known that linear beam elongation is proportional to the average temperature and conditions that limit its free movement. Then the obvious equality can be derived:

$$U(L,t) = \beta \cdot K \cdot \int_0^L T(x,t)\,dx = \beta \cdot K \cdot L \cdot T_{\varnothing}(L,t) = L^0 \cdot T_{\varnothing}(L,t)\,; \quad (1)$$

where β - the coefficient of linear elongation of the beam material, K - the coefficient characterizing the conditions for limiting the free expansion of the beam, L - the length of the beam, $T_{\varnothing}(t)$ - the average temperature along the beam length, $L^0 = \beta \cdot K \cdot L$. The average core temperature $T_{\varnothing}(t)$ is determined when the function of temperature change $T(x,t)$ along the length of the beam is known:

$$T_{\varnothing}(t) = L^{-1} \cdot \int_0^L T(x,t)\,dx.$$

Consequently, the thermoelastic structure can be determined as follows, with the position matrix Mi, the linear model of TCP displacement of the machine tool, which examines the linear relationship between the output parameter $\delta r = |\delta r_x \delta r_y \delta r_z 1|^T$ and the linear temperature shifts of the thermally active elements $\delta r_i^0 = |\delta r_{ix}^0 \delta r_{iy}^0 \delta r_{iz}^0 1|^T$ only due to their average excess temperatures [Kuznetsov 2018]:

$$\delta r = \sum_{i=1}^{n-1}(\prod_{i=1}^{n-(i+1)} M_i) \times K_i \times \delta r_i^0 = \sum_{i=1}^{n-1}(\prod_{i=1}^{n-(i+1)} M_i) \times L_i^0 \times T_{\varphi i}^0 = M_1 \times M_2 \times M_3 \times M_4 \times M_5 \times L_1^0 \times T_{\varphi 1}^0 + M_1 \times M_2 \times M_3 \times M_4 \times L_2^0 \times T_{\varphi 2}^0 + M_1 \times M_2 \times M_3 \times L_3^0 \times T_{\varphi 3}^0 + M_1 \times M_2 \times L_4^0 \times T_{\varphi 4}^0 + M_1 \times L_5^0 \times T_{\varphi 5}^0(t) + L_6^0 \times T_{\varphi 6}^0\,; \quad (2)$$

The change in time of the machine tool TCP shift is determined by the following equation for the conditions of heat exchange and constancy (not accidental) of the machine tool's thermal loads according to [Kuznetsov 2018]:

$$\delta r(t) = \sum_{i=1}^{n-1}(\prod_{i=1}^{n-(i+1)} M_i) \times k_i \times T_{\varphi i}^0(1 - e^{-m_{vi} \cdot t})\,; \quad (3)$$

where $m_{vi} \cdot t = K_g^{-1} \cdot K_g^y \cdot Bi \cdot Fo \cdot \psi$ - temperature change rate, K_g , K_g^y - coefficients of geometric similarity; Bi - Biot and Fo Fourier similarity criteria; ψ - coefficient of temperature irregularity. The type and form of regularities of TCP change for machine tools are justified and given in [Kuznetsov 2018].

If the temperature field distribution is uniform, then $\psi = 1\ and\ Bi_v \to 0$. Furthermore, the higher the unevenness of the temperature field, the smaller the value $\to 0$, and the higher the value $Bi_v \to \infty$. Consequently, the Biot criterion characterizes the condition and degree of non-uniformity of the temperature field. Thus, for practical applications, if the Biot criterion value is below 0.1, the temperature field is close to uniform and in this case, for example, there will be no bending. At Biot numbers greater than 0.1 the temperature field is non-uniform, which will cause thermal bending deformations.

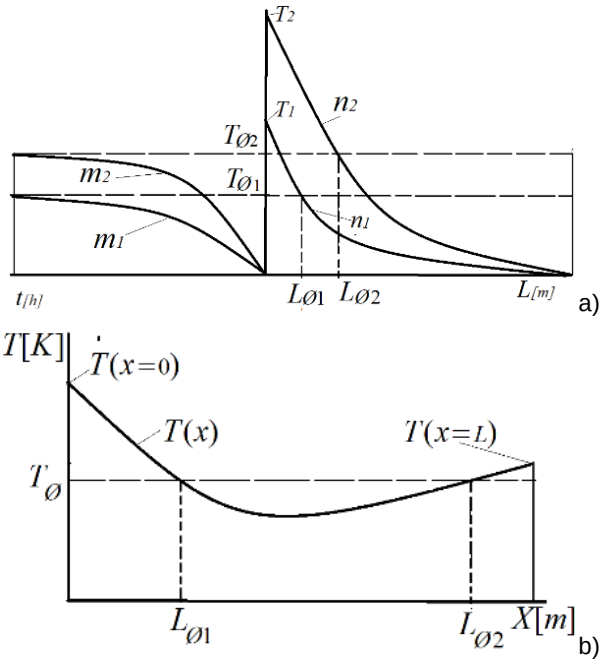

Fig. 1 Typical diagrams of temperature changes along the length of the thermally active element: a) along the length with *one heating source of different intensity T₁ and T₂ b) for two heating sources.*

The temperature of a thermally active beam element ($Bi_v \ll 0.1$) of the machine tool (spindle, ball screw, beam, plate in the form of an edge, beam of arbitrary cross-section) will undergo a characteristic change in the length of such an element, as it is shown in Fig. 1. The heating temperature ($T_1 > T_2$) and average temperature ($T_{\varnothing 1} > T_{\varnothing 2}$) of a thermally active element will differ for different conditions of heat exchange and heat supply. The speed of temperature change ($m_1 > m_2$) for different spindle speeds ($n_1 > n_2$) will also differ (see Fig. 1a). In this case, the intersection points of functions $T(x,t)$ and $T_{\varnothing}$ in general will be different $L_{\varnothing 1} \neq L_{\varnothing 2}$ for different thermal loads. Therefore, understanding this allows the justification of both the location of sensors and their required number, and perhaps even the achievable accuracy of numerical compensation, the choice of control method, efficiency, cost and complexity of such a system.

2.2 Thermal design of spindle units

In order to substantiate the location of the sensors and their number for the machine's temperature error compensation systems, spindle assemblies will be considered as an example of a typical core machine component, as they are characteristic representatives of a group of thermally active elements (spindle, ball screw, beam, plate, rod of any cross-section). Structurally, spindle assemblies can be characterized by the distance between the supports, the type of support used, the size of the spindle, the presence of an internal hole, the placement of drive elements, the method of fixing the chuck for the part or tool, the requirements for accuracy, etc.

Analyzing spindle unit designs of machine tools for the tasks of their thermophysical design allowed the systematization of typical external and internal forms. The spindle surface is divided in two types of groups of structural shape: the *first group* represents the typical external forms of the spindle, which can be smooth cylindrical, with a flange end or step with a small number of steps; the *second group* includes the typical internal forms of the spindle.

Tab. 1 Thermal spindle models.

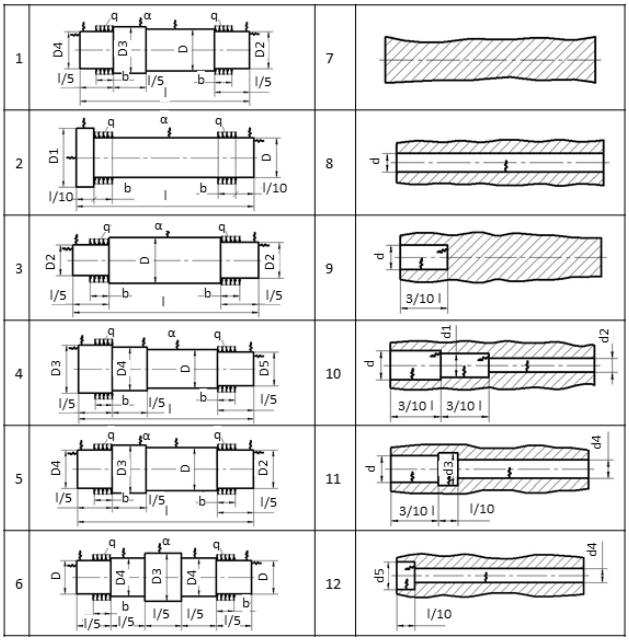

Table 1 shows characteristic thermal models of spindles. A thermal spindle model is a solid or hollow cylinder with constant or variable cross-section, on the outer and inner surfaces of which there is a heat exchange with the environment with the coefficient of heat convection α. Each surface may have different heat convection coefficients and values due to different heat flow conditions with the environment. For example, the heat convection conditions on the surfaces of the protruding part of the spindle may be very different from the heat convection conditions on the inner surface of the spindle, where the heat exchange with the environment is much more difficult. Heat flow to the spindle surface is carried out from different sources of heat: spindle supports, drive elements, tools or parts that are attached to the spindle and are heated by heat generation during cutting. In general, the diameter of the thermal model cylinder $d_{\varnothing}$ is determined on based on the equality of Biot and Fourier similarity criteria and is determined as follows:

$$d_{\varnothing} = \frac{\alpha_{\varnothing}\left(\sum d_i^2 l_i - \sum d_j^2 l_j\right)}{\left(\sum \alpha_i d_i l_i + \sum \alpha_j d_j l_j + \sum \alpha_{\tau i}(d_i^2 - d_j^2)\right)}; \quad (4)$$

where $\alpha_{\varnothing}$ is the accepted heat convection coefficient of the thermal model or calculated according to dependence

$$\alpha_{\varnothing} = \frac{\sum(\alpha_i A_i) + \sum(\alpha_{\tau j} A_{\tau j})}{\sum(A_i) + \sum(A_{\tau j})}; \quad (5)$$

where α_i is the heat convection coefficient of the heat convection surface Ai (internal and external), $\alpha_{\tau i}$ is the heat convection coefficient of end surfaces.

When it is necessary to consider the heat convection from the end surface, the length L_{Ti} is used instead of the length L of the spindle:

$$L_{Ti} = L + \frac{\alpha_m}{\alpha} \cdot \frac{A}{P}; \quad (6)$$

where P is the perimeter of a cylinder or beam of any cross-section. The Nusselt number of the outer surface for rotating spindles, ball screws, and shafts is calculated by:

$$\overline{Nu} = 0.18[(0.5\,Re^2 + Gr)Pr]^{0.315} = 0.18\left[\left(0.5\left(\frac{\pi d^2 n}{60\nu}\right)^2 + \frac{g\beta\Delta T d^3}{\nu^2}\right)Pr\right]^{0.315} = 0.18\left[\frac{d^4 n^2}{\nu^2}\left(0.5\left(\frac{\pi}{60}\right)^2 + \frac{g\beta\Delta T}{dn^2}\right)Pr\right]^{0.315}; \quad (7)$$

Conversion of this equation allowed obtaining the value of heat convection coefficient, which is a function of speed and diameter. After simplifications for $d > 0.03\,m$ and $n > 150 min^{-1}$ with an error of no more than 1.5%, it is possible to record the heat convection coefficient:

$$\alpha = \frac{0.18\cdot\lambda}{\nu^{2\cdot 0.315}} \cdot Pr^{0.315}\left[0.5\left(\frac{\pi}{60}\right)^2 + \frac{g\beta\Delta T}{dn^2}\right]^{0.315} \cdot d^{4\cdot 0.315-1} \cdot n^{2\cdot 0.315} = 0.551 \cdot d^{4\cdot 0.315-1} \cdot n^{2\cdot 0.315} = 0.551 \cdot d^{0.26} \cdot n^{0.63}; \quad (8)$$

Analyzing equation (8) allows for the conclusion that the range of variation of the heat convection coefficient for different values of rotation speeds and diameters lies in the range of 11÷105 [W/m²·K].

2.3 Temperature models

A thermal model is a spindle sketch, drawn without any structural features (chamfers, grooves, radii of curvature, etc.), where continuous thin lines depict the boundaries of the active zones of heat sources and the boundaries of areas within which the heat exchange coefficient between the spindle and the environment or other thermophysical characteristics can be assumed as constant. The mathematical description of the process of stationary thermal spindle conductivity is a differential equation with boundary conditions of the second kind, which is generally determined as follows:

$$\lambda\frac{\partial^2 T(x)}{dx} = 0;\ \lambda\frac{\partial T(x)}{dx} + \alpha|_{A_2} T(x) + q(x)|_{A_1} = 0; \quad (9)$$

where λ - is the heat conduction coefficient; α is the heat convection coefficient; A_2 - boundary surface, on which α is set; $q(x)$ - function of heat flow density; A_1 - boundary surface, on which the heat flow density is set; $A_1 \cup A_2$ - full spindle surface. The peculiarities of the formulated task comprise the complexity of heat exchange conditions on the A_2 surface of the thermal model, the variety of geometric shapes adopted in thermal models $A_1 \cup A_2$, and the uncertainty in the number and location of heat sources. The dimensions of all spindles were derived from the average spindle size. The following main dimensions were used (see Tab. 1): outer diameter $D = 80\,mm$; inner diameter $d = 50\,mm$; spindle spacing $L_0 = 350\,mm$; spindle length $L = 500\,mm$. The following sizes of the spindle's external and internal structural forms were chosen with regard to these sizes: $D_1 = 150\,mm$, $D_2 = 70\,mm$, $D_3 = 90\,mm$, $D_4 = 85\,mm$, $D_5 = 75\,mm$, $d_1 = 50\,mm$, $d_2 = 45\,mm$, $d_3 = 40\,mm$, $d_4 = 55\,mm$, $d_5 = 35\,mm$, $d_6 = 35\,mm$.

For subsequent comparative analysis of the calculation results, the thermal models were put in the same conditions

of heat exchange and thermal loading. For all thermal models, equal values were taken for heat convection coefficients on external, internal, and end surfaces, for thermophysical parameters of spindle material, and values of heat flow: $\alpha = 5\ W/m^2K$; $q = 1\ W/m^2$; $\lambda = 40\ W/m \cdot K$. These initial data were used to calculate the nodal values of temperatures along the spindle axis, and for its maximum and average temperatures. Fig. 2 shows the results of these calculations for design forms in Tab.1.

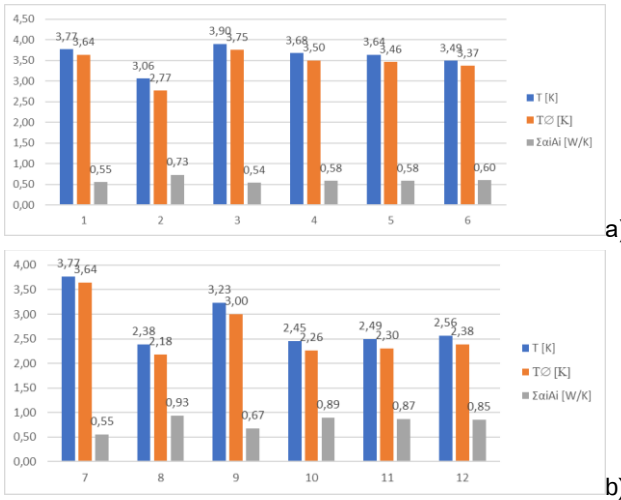

Fig. 2 Temperature characteristics of spindles of various a) external and b) internal design forms in Tab.1.

While all other conditions remaining equal, geometric parameters of the external and internal spindle forms have a significant impact on thermal spindle characteristics. Thus, for external forms, the relative change of average and maximum temperatures is 25 and 20%, respectively, and for various internal forms, it is -41 and 37%. Obviously, such significant spreads (from 20 to 37%) of values of both average temperatures and maximum temperatures lead to a significant error. Proportional to this change, in the control systems of temperature performs TCP shift compensation, which is essential for this task definition. Therefore, it is necessary to perform a more in-depth analysis of the parameters that determine the changes in the mean excessive temperatures and affect their location along the spindle length by using analytical methods.

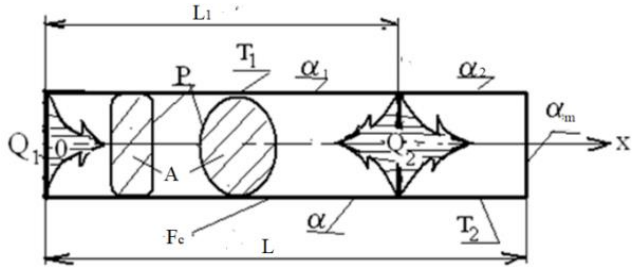

Fig. 3 Thermal model of spindle assembly with free surface of heat exchange at front bearing.

3 COMPARISON OF METHODS

For this purpose, a generalized thermal model is considered (Fig. 3). Such a model with the given parameters in accordance with the criteria of similarity of thermal physical processes allows building other models by changing the position and types of thermal loads.

3.1 Analytical method

It is necessary to obtain an analytical solution for the following conditions of heat exchange: 1 - heat supply is carried out through the end faces with a constant coefficient of heat exchange through the side surface; 2 - heat supply is carried out through the end faces of the Q_1 spindle rear support, Q_2 front support surface with a constant α and different (α_1 and α_2) coefficients of heat convection through the free side faces; 3 - heat supply is carried out through the end faces of the Q_1 spindle rear support, Q_1 front support surface. For the first case, an explicit equation was obtained to determine the spindle temperature:

$$T(x) = \frac{Q_2}{A\lambda m} \cdot \frac{\cosh(mx)}{\sinh(mL)} + \frac{Q_1}{A\lambda m} \cdot \frac{\cosh[m(L-x)]}{\sinh(mL)}; \quad (10)$$

The average spindle temperature is defined as follows:

$$T_{\varnothing} = \frac{1}{L}\int_0^L \frac{Q_2}{A\lambda m} \cdot \frac{\cosh(mx)}{\sinh(ml)} + \frac{Q_1}{A\lambda m} \cdot \frac{\cosh[m(L-x)]}{\sinh(mL)} dx = \frac{1}{L} \cdot \frac{Q_2}{A\lambda m} \cdot \frac{1}{\sinh(ml)} \cdot \frac{1}{m}[\sinh(mL) - \sinh(0)] + \frac{1}{L} \cdot \frac{Q_1}{A\lambda m} \cdot \frac{1}{\sinh(ml)} \cdot [-\frac{1}{m}][\sinh(m \cdot 0) - \sinh(mL)] = \frac{1}{L} \cdot \frac{Q_2}{A\lambda m} \cdot \frac{1}{m} + \frac{1}{L} \cdot \frac{Q_1}{A\lambda m} \cdot \frac{1}{m} = \frac{1}{4\alpha} \cdot \frac{d}{L} \cdot \frac{1}{A}(Q_1 + Q_2) = \frac{1}{\alpha} \cdot \frac{1}{A_c} \cdot (Q_1 + Q_2) = \frac{Q_1+Q_2}{L \cdot m \cdot (A \cdot \lambda \cdot m)}; \quad (11)$$

where $m^2 = \frac{4 \cdot \alpha}{\lambda \cdot d}$.; $A_c = L \cdot P$.

Based on the equality of equations (10) and (11) $T_{\varnothing} = T(x)$, the x_i coordinates along the spindle length are found, where the absolute temperature will be equal to the average temperature of the spindle. For this reason, the specified equation is converted to the following form:

$$T_{\varnothing} = \frac{Q_1}{A \cdot \lambda \cdot m} \cdot \frac{cosh[m \cdot (L-x)]}{sinh(m \cdot L)} + \frac{Q_2}{A \cdot \lambda \cdot m} \cdot \frac{cosh(m \cdot x)]}{sinh(m \cdot L)} = \frac{1}{2 \cdot A \cdot \lambda \cdot m \cdot sinh(m \cdot L)} \cdot [Q_1 \cdot (e^{m \cdot (L-x)} + e^{-m \cdot (L-x)}) + Q_2 \cdot (e^{m \cdot x} + e^{-m \cdot x})];$$

$$2 \cdot A \cdot \lambda \cdot m \cdot sinh(m \cdot L) \cdot T_{\varnothing} \cdot e^{m \cdot x} = Q_2 + Q_1 \cdot e^{m \cdot l} + e^{m \cdot x} \cdot e^{m \cdot x} \cdot (Q_2 + Q_1 \cdot e^{-m \cdot L}); \quad (12)$$

Entering the designations: $2 \cdot A \cdot \lambda \cdot m \cdot \sinh(m \cdot L) = a$; $(Q_2 + Q_1 e^{m \cdot L}) = c$; $(Q_2 + Q_1 e^{-m \cdot L}) = b$; and $e^{m \cdot x} = y$; results in the equation of the solution:

$$y = \frac{a \cdot T_{\varnothing} \pm \sqrt{(a \cdot T_{\varnothing})^2 - 4bc}}{2b}. \quad (13)$$

Consequently, the coordinates $x_{1,2}$ are spindle points where the temperature values $T(x)$ are equal to the average $T_{\varnothing}$:

$$x_{1,2} = \frac{1}{m} \cdot ln \frac{\frac{Q_1+Q_2}{L \cdot m} \cdot \sinh(m \cdot l) \pm \sqrt{[\frac{(Q_1+Q_2)}{L \cdot m} \cdot \sinh(m \cdot L)]^2 - [Q_2^2 + 2 \cdot Q_1 Q_2 \cdot \cosh(m \cdot L) + Q_1^2]}}{[Q_2 + Q_1 e^{-m \cdot L}]}; \quad (14)$$

In order to ensure comparability of the results, the initial data for spindle temperature determination are adopted as follows for all types of subsequent calculations:

- Heat emission in the rear spindle support $Q_1 = 25\ W$,
- Heat dissipation at the front spindle support $Q_2 = 45\ W$,
- Spindle length $L = 0.5\ m$,
- Spindle equivalent model diameter $d_{\varnothing} = 0.1\ m$,
- Distance between front and rear supports $L_1 = 0.4\ m$,
- Spindle heat convection coefficient $\alpha = 25\ W/m^2 \cdot K$,
- Spindle heat conduction coefficient $\lambda = 40\ W/m \cdot K$.

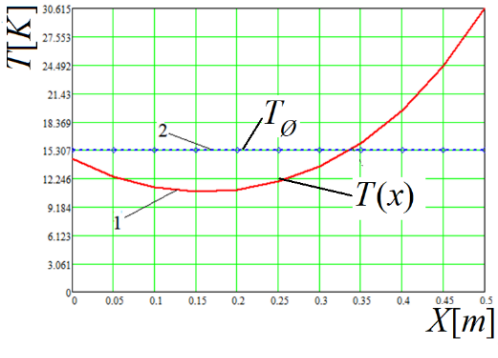

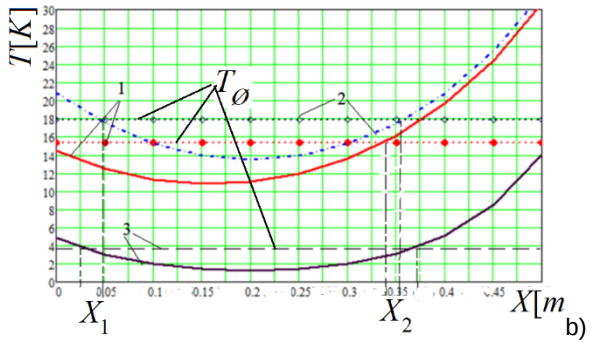

Fig. 4 a)Temperature change along spindle length 1 and average temperature 2 and coordinates; b) coordinates $x_{1,2}$ for different heat exchange conditions.

Fig. 4 shows graphs of the spindle temperature change $T(x)$ and the location of the intersection point, where the temperature value at a distance x is equal to the average $T_{\varnothing}$. This result corresponds to the scheme of Fig. 2b but has only one coordinate of temperature equality, which confirms the assumption about the materiality of the temperature sensor's location in the correction control system using these data.

For general initial data from (11), it is determined that $T_{\varnothing} = 15.28$, $x_1 = -0.017\,m$, $x_2 = 0.336\,m$ ("1" in Fig. 4b), and other conditions being equal, but only $Q_1 = 25\,W$ will change, then $T_{\varnothing} = 17.825$, $x_1 = 0.044\,m$, $x_2 = 0.412\,m$ ("2" in Fig. 4b) and at $Q_1 = 35\,W$: $T_{\varnothing} = 20.372$, $x_1 = 0.08\,m$, $x_2 = 0.377\,m$, and if only $\alpha = 105 W/m^2 \cdot K$ changes, then $T_{\varnothing} = 3.638$, $x_1 = 0.029\,m$, $x_2 = 0.365\,m$ ("3" in Fig. 4b), and if $Q_1 = 35\,W$ and $\alpha = 105\,W/m^2 \cdot K$, then $T_{\varnothing} = 4.85$, $x_1 = 0.084\,m$, $x_2 = 0.392\,m$.

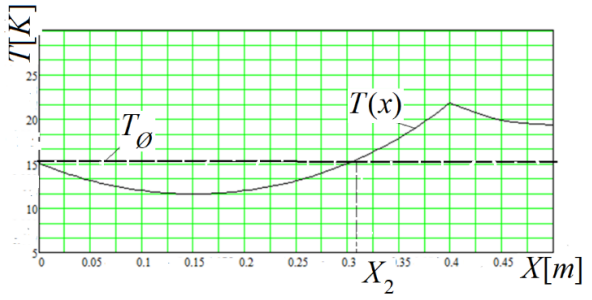

Fig. 5 Temperature variation along spindle length and average temperature for the second case of the thermal model.

Then, for the above initial data, Fig. 5 shows a graph of temperature changes along the spindle length obtained by equations (15) and (16), and the average spindle temperature. Considering that the function of temperature change T_1 is dominating in the analysis of components for the model's adopted thermophysical parameters, the subsequent dependence of temperature change for the considered models will be determined only for this function.

The following input data for spindle temperature determination are used for all types of models in the following calculations: heat dissipation at the back of the spindle $Q_1 = 15\,W$; heat dissipation at the front of the spindle $Q_2 = 45\,W$; spindle length (or given length) $L = 0.5\,m$; spindle diameter (or equivalent model diameter) $d_{\varnothing} = 0.1\,m$; distance between the front and rear supports $L_1 = 0.4\,m$; spindle heat convection coefficient $\alpha = 25\,W/m^2 \cdot \mathrm{K}$; spindle material heat conduction coefficient $\lambda = 40\,W/m \cdot \mathrm{K}$.

For the second case of the thermal model, the heat is supplied from a bearing located at the end of the spindle (rear spindle support) Q_1, and from a bearing (front spindle support) Q_2, the distance between which is L_1. Moreover, the heat exchange with the environment takes place on the cylindrical surface of the spindle between the bearings and on the free surface (spindle shaft journals) at a distance of (L - L_1) from the front bearing to the free end with the same and equal coefficients of heat convection α, and the end surface is insulated $\frac{\partial T_2}{\partial x}|_{x=L} = 0$, which results in the following solution for the temperature distribution along the length of the rod:

$$T_1(x) = \frac{Q_2}{A \cdot m \cdot \lambda} \cdot \frac{\tanh^{-1}[m \cdot (L - L_1)]}{1 + \tanh^{-1}[m \cdot (L - L_1)] \cdot \tanh(m \cdot L_1)} \cdot \frac{\cosh(m \cdot x)}{\cosh(m \cdot L_1)} + \frac{Q_1}{A \cdot m \cdot \lambda} \cdot \frac{[\cosh(m \cdot L_1) - \sinh(m \cdot L_1)]\{\tanh^{-1}[m \cdot (L - L_1)] - 1\}}{\{1 + \tanh^{-1}[m \cdot (L - L_1)] \cdot \tanh(m \cdot L_1)\}} \cdot \frac{\cosh(m \cdot x)}{\cosh(m \cdot L_1)} + \frac{Q_1}{A \cdot m \cdot \lambda} \cdot [\cosh(m \cdot x) - \sinh(m \cdot x)]; \quad (15)$$

$$T_2 = \frac{1}{A \cdot m \cdot \lambda} \cdot \left(\frac{Q_2 \cdot \left(\frac{d}{e}\right)}{d\left[1 + \left(\frac{d}{e}\right) \cdot \tanh(m \cdot L_1)\right]} - \frac{Q_1 \cdot e^{-m \cdot L_1} \cdot \left[1 - \left(\frac{d}{e}\right)\right]}{d\left[1 + \left(\frac{d}{e}\right) \cdot \tanh(m \cdot L_1)\right]} + \frac{Q_1 \cdot e^{-m \cdot L_1}}{d} \right) \cdot (e^{m \cdot x} + e^{2m \cdot L} \cdot e^{-m \cdot x}); \quad (16)$$

where:

$$d = e^{m \cdot L_1} \cdot [1 + e^{2m \cdot (L - L_1)}]; \; e = e^{m \cdot L_1} \cdot [e^{2m \cdot (L - L_1)} - 1];$$

$$T_{\varnothing 1} = \frac{1}{L_1} \cdot \frac{Q_2}{A \cdot m \cdot \lambda} \cdot \frac{\tanh^{-1}[m \cdot (L - L_1)]}{1 + \tanh^{-1}[m \cdot (L - L_1)] \cdot \tanh^{-1}(m \cdot L_1)} \cdot \frac{1}{m} \cdot \frac{\sinh(m \cdot L_1)}{\cosh(m \cdot L_1)} + \frac{1}{L_1} \cdot \frac{Q_1}{A \cdot m \cdot \lambda} \cdot \frac{[\cosh(m \cdot L_1) - \sinh(m \cdot L_1)] \cdot \{\tanh^{-1}[m \cdot (L - L_1)] - 1\}}{\{1 + \tanh^{-1}[m \cdot (L - L_1)] \cdot \tanh(m \cdot L_1)\}} \cdot \frac{1}{m} \cdot \frac{\sinh(m \cdot L_1)}{\cosh(m \cdot L_1)} + \frac{1}{L_1} \cdot \frac{Q_1}{A \cdot m \cdot \lambda} \cdot \frac{1}{m} \cdot [\sinh(m \cdot L_1) - \cosh(m \cdot L_1) + 1]; \quad (17)$$

$$T_{\varnothing 2} = \frac{1}{L - L_1} \cdot \frac{1}{A \cdot m \cdot \lambda} \cdot \left\{ \frac{Q_2 \cdot (d/e)}{d \cdot [1 + (d/e) \cdot \tanh(m \cdot L_1)]} - \frac{Q_1 \cdot [1 - (d/e)] \cdot e^{-m \cdot L_1)}}{d \cdot [1 + (d/e) \cdot \tanh(m \cdot L_1)]} + \frac{Q_1 \cdot e^{-m \cdot L_1)}}{d} \right\} \cdot \frac{1}{m} \cdot [e^{m \cdot L} - e^{m \cdot L_1} - e^{2m \cdot L} \cdot (e^{-m \cdot L} - e^{-m \cdot L_1})]; \quad (18)$$

$$T_{\varnothing} = \frac{L_1}{L} \cdot T_{\varnothing 1} + \frac{L - L_1}{L} \cdot T_{\varnothing 2} = \frac{1}{L} \cdot [L_1 \cdot T_{\varnothing 1} + (L - L_1) \cdot T_{\varnothing 2}]; \quad (19)$$

Equations (17 -19) can be written as follows in a more general uniform form:

$$T_{\varnothing} = \frac{1}{L} \cdot \frac{Q_2}{A \lambda m} \cdot \frac{1}{m} \cdot K_{Q2} + \frac{1}{L} \cdot \frac{Q_1}{A \lambda m} \cdot \frac{1}{m} K_{Q1}; \quad (20)$$

K_{Q1} and K_{Q2} - coefficients of change of maximum temperatures in places of heat supply and the nature of temperature changes along the spindle length, due to the parameters and type of heat exchange.

The initial data comprise $T_{\varnothing} = 15.22$, temperatures in the bearing supports $T_1 = 15.02$ and $T_2 = 21.87$. Consequently, only one point on the spindle length will be equal to the average and current spindle temperature. So, for the thermal model, when coefficients of heat exchange through the free side surfaces are different (α_1 and α_2), this leads to:

$$T_1(x) = \frac{Q_2}{A \cdot m_2 \cdot \lambda} \cdot \frac{\tanh^{-1}[m_2 \cdot (L - L_1)]}{1 + \frac{m_1}{m_2} \cdot \tanh^{-1}[m_2 \cdot (L - L_1)] \cdot \tanh(m_1 \cdot L_1)} \cdot \frac{\cosh(m_1 \cdot x)}{\cosh(m_1 \cdot L_1)} + \frac{Q_1}{A \cdot m_1 \cdot \lambda} \cdot \frac{[\cosh(m_1 \cdot L_1) - \sinh(m_1 \cdot L_1)]\{\tanh^{-1}[m_2 \cdot (L - L_1)] - \frac{m_1}{m_2}\}}{\{1 + \frac{m_1}{m_2} \cdot \tanh^{-1}[m_2 \cdot (L - L_1)] \cdot \tanh(m_1 \cdot L_1)\}} \cdot \frac{\cosh(m_1 \cdot x)}{\cosh(m_1 \cdot L_1)} + \frac{Q_1}{A \cdot m_1 \cdot \lambda} \cdot [\cosh(m_1 \cdot x) - \sinh(m_1 \cdot x)]; \quad (21)$$

The average temperature will be determined by equation (20), under the corresponding conditions of heat exchange values K_{Q1} and K_{Q2} - coefficients of change of maximum temperatures in places of heat supply and the nature of temperature changes along the spindle length, due to the parameters and type of heat exchange.

In all cases of changing heat exchange conditions with parameters exceeding the initial model, the value of these

coefficients is below one. For the third case, the heat flow model is carried out through the end faces of the Q_1 spindle rear support, the Q_2 front support surface with a constant α and different (α_1 and α_2) coefficients of heat flow through the free side faces and the end face (α_t) of the temperature distribution, e.g., T_1 will be calculated as follows:

$$T_1(x) = \frac{Q_2}{A \cdot m_2 \cdot \lambda} \cdot \frac{D_T}{1+\frac{m_1}{m_2} \cdot D_T \cdot \tanh(m_1 \cdot L_1)} \cdot \frac{\cosh(m_1 \cdot x)}{\cosh(m_1 \cdot L_1)} + \frac{Q_1}{A \cdot m_1 \cdot \lambda} \cdot \frac{[\cosh(m_1 \cdot L_1) - \sinh(m_1 \cdot L_1)] \cdot [\frac{m_1}{m_2} \cdot D_T - 1]}{1+\frac{m_1}{m_2} \cdot D_T \cdot \tanh(m_1 \cdot L_1)} \cdot \frac{\cosh(m_1 \cdot x)}{\cosh(m_1 \cdot L_1)} + \frac{Q_1}{A \cdot m_1 \cdot \lambda} \cdot [\cosh(m_1 \cdot x) - \sinh(m_1 \cdot x)]; \quad (22)$$

with: $D_m = \frac{[K_m \cdot e^{2(L-L_1) \cdot m_2} + 1]}{[K_m \cdot e^{2(L-L_1) \cdot m_2} - 1]}$; $K_m = \frac{[m_2 + (\alpha_m/\lambda)]}{[m_2 - (\alpha_m/\lambda)]}$.

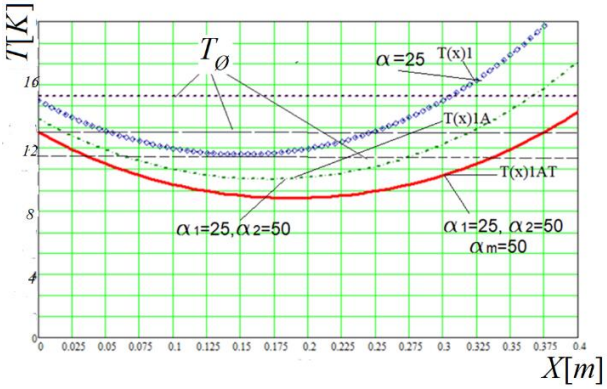

Fig. 6 Temperature variation along spindle length, and average temperature for the thermal model.

The average temperature will also be determined by equation (20), under the corresponding conditions of heat exchange K_{Q1} and K_{Q2}. It follows that the place's position along the length of the spindle varies from one to two points.

The distance also varies widely from 5 to 35%, which most directly affects the accuracy of the computed model of compilation according to equation (2), which is similar in structure to the correlation and regression models used by different researchers. Thus, it can be argued that the existing models of TCP temperature deformation correction systems already contain an error in advance. The error is not less than the one obtained from this investigation. These models are uncertain in terms of choice of place and number of measurement points. Thus, these existing models are limited to some extent, based on the required accuracy of the correction result.

3.2 FEM method

In addition to the considered methods, the applicability of the FEM was analyzed for the specified purposes of the measured temperature correction in multiple points. The basic idea of FEM is that any continuous value such as temperature can be approximated by a discrete model on a set of piecewise continuous functions defined by a finite number of subareas. For this purpose, the typical spindle model is divided into a finite number of regions, called finite elements. The partitioning is performed in planes perpendicular to the spindle axis so that the geometrical cross-section dimensions, loading conditions and heat exchange remain constant (without jumps) for each finite element.

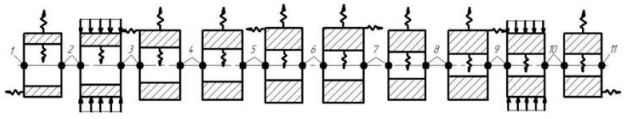

Fig. 7 Breakdown of spindle's thermal model.

Fig. 7 shows an example of the spindle's thermal model partition. The nodal points that common to the neighboring finite elements are selected at the intersection of the partition planes with the spindle axis.

Since FEM belongs to the approximate methods of solving the problems of heat conductivity, it requires justification and confirmation by comparing the results obtained with those of analytical heat calculations. A finite length cylinder L is used as a thermal model for comparative calculations. On the flange surfaces of this cylinder, heat is exchanged with the environment with a heat convection coefficient α. Heat is supplied to the cylinder through one end face surface, and on the other end face surface the heat flow is zero. A comparison of the FEM solution and the analytical one for determining the temperature field of the considered thermal model, obtained as a special case of the solution (11,15, 21), showed that the error is not uniform and is approx. 3% when divided into more than 100 finite elements and in comparison with the experiments, up to 11-14%.

Determining the number of finite elements is necessary to obtain the spindle temperature. The application of correlation dependences for correcting temperature deformations is based on revealing the connection of measured temperatures and the machine elements' values of average temperature, as temperature displacements are proportional to these average temperatures.

3.3 Accuracy of methods and sensor locations

The aim is to reduce the number of measurement points from which these average temperatures can be calculated. The more measurement points, the more accurately the average temperature is determined, and accordingly, the deformations of the machine and its components are also more accurate. However, the aim is to reduce the number of such measurement points in order to reduce the computational effort, the complexity of the whole measurement system, its structural complexity, which implies reducing its cost.

Then, this task can be compared with determining the number of finite elements, the value of which determines the accuracy of the approximation function of temperature change, which determines the average temperature of the machine parts. The number of finite elements is not very critical for temperature calculations, and it can practically be realized in a sufficiently large volume measured from hundreds and thousands of elements to tens and hundreds of thousands. Therefore, the number of measurement locations in the machine tools is limited and cannot be similar to the large amount of finite elements in the calculations. Therefore, it is necessary to define a number of control points that will allow approximating the function with a given accuracy, which is similar to the solution of the task of determining the number of finite elements in order to achieve the same accuracy of approximation.

On the one hand, it should be considered that the accuracy of calculations is higher with a higher number of finite elements. On the other hand, with increasing number of finite elements, the dimensionality of the system of linear equations increases, and, consequently, the requirements increase regarding the applied means of computer technology (memory capacity, performance). With the same amount of memory, the calculation performance (speed of calculations) drops rapidly with increasing number of finite elements. In the literature on FEM applications, recommendations are given on the choice of the number of finite elements, which consists in the fact that in places with the highest temperature gradients, the partition frequency should be higher than in places with low thermal loads. On the one hand, the elements must be

chosen small enough to make the results acceptable, and on the other hand, the use of sufficiently large elements reduces the computational work. Therefore, some criteria are required to regulate the number of elements so that it is possible to reduce their size in areas where the expected result can vary strongly, or to increase them where the expected result is almost constant. Thus, the number of elements is a matter of choice, not of defining or estimating the number of finite elements, which is not a sufficiently strict and objective rule and depends on skills in working on a relatively narrow range of similar tasks.

The first line of the system of linear equations, based on the values of the stiffness matrix and loads obtained in [Kuznetsov 2019], will be written in the following form:

$$T_1 \cdot \left(\frac{A\lambda N}{L} + \frac{2\pi dL\alpha}{6N}\right) + T_2 \cdot \left(\frac{\pi dL\alpha}{6N} - \frac{A\lambda N}{L}\right) = Q_1 + \frac{\pi dL\alpha T_0}{2N}\ ; \quad (23)$$

where T_0 - ambient temperature. Denote: $K_1 = \frac{A\lambda}{L}$; $K_2 = \frac{\pi dL\alpha}{6}$; $K_3 = \frac{\pi dL\alpha T_0}{2}$. Then equation (23) will be written after a transformation and considering the accepted notation:

$$K_1 N \cdot (T_1 - T_2) + \frac{K_2}{N} \cdot (2T_1 + T_2) = Q_1 + \frac{K_3}{N}\ ; \quad (24)$$

The temperature difference between the initial and final points of the element is marked $E = T_1 - T_2$, and their ratio $T_1/T_2 = \varepsilon$. If the number of finite elements is infinitely large $(N \to \infty)$, the temperature difference between the initial and final points of the element will tend to zero. This is also derived from equation (24) when substituting the value of $N = \infty$ into it:

$$K_1 \cdot (T_1 - T_2) + \frac{K_2}{N^2} \cdot (2T_1 + T_2) = \frac{Q_1}{N} + \frac{K_3}{N^2}\ ; \quad (25)$$

where $N = \infty$; $K_1(T_1 - T_2) = 0$; since K_1 is always above zero, then $T_1 - T_2 = 0$. Consequently, the temperature difference can be accepted as an initial parameter, the number of finite elements N depends on its value. Therefore, solving equation (24) with respect to N results in the value of the number of finite elements, based on the admissible temperature difference between the initial and final points of the element:

$$N = \frac{Q_1 + \sqrt{Q_1^2 - 4K_1E\left[K_2E\left(\frac{2\varepsilon+1}{\varepsilon-1}\right) - K_3\right]}}{2K_1E}\ ; \quad (26)$$

Considering the previously accepted designations, the number of finite elements will be calculated as follows:

$$N = \frac{Q_1L + L\sqrt{Q_1^2 - 2A\lambda\pi d\alpha E\left[E\left(\frac{2\varepsilon+1}{3\varepsilon-3}\right) - T_0\right]}}{2A\lambda E}\ ; \quad (27)$$

The second and subsequent lines of the system of linear equations have the same structure, so it is suggested to write down and analyze only the second line, which will be determined as follows, after the transformation and the introduction of the previously adopted notation:

$$EK_1N + \frac{K_2}{N} \cdot \left(\frac{2\varepsilon+1}{\varepsilon-1}\right)E = \frac{K_3}{N}\ ; \quad (28)$$

Solving equation (28) relative to N results in:

$$N = \sqrt{\frac{K_3 - K_2E \cdot \left(\frac{2\varepsilon+1}{\varepsilon-1}\right)}{K_1E}}\ ; \quad (29)$$

or subject to accepted designations

$$N = L\sqrt{\frac{\pi d\alpha}{2F\lambda E} \cdot \left[T_0 - E \cdot \left(\frac{2\varepsilon+1}{3\varepsilon-3}\right)\right]}\ ; \quad (30)$$

The comparison of equations (27) and (30) shows that they have the same structure, and the increase in the number of finite elements in places of thermal stress is only due to this load. Therefore, equation (27)leads to equation (30). Then, by entering the designation

$$N_0 = \sqrt{\frac{\pi d\alpha}{2F\lambda E} \cdot \left[T_0 - E \cdot \left(\frac{2\varepsilon+1}{3\varepsilon-3}\right)\right]}\ ; \quad (31)$$

the following equations result for estimating the number of finite elements in determining the spindle temperature field:

- in the presence of thermal stress on the element:

$$N_q = L \cdot \frac{Q_1}{2A\lambda E} + L \cdot \sqrt{\left(\frac{Q_1}{2A\lambda E}\right)^2 + N_0^2}\ ; \quad (32)$$

- in the absence of heat load on the element:

$$N_L = L \cdot N_0\ ; \quad (33)$$

For example, it is necessary to determine the number of finite elements for the following input data: $Q_1 = 10$; $K_1 = 0.63$; $K_2 = 0.13$; $K_3 = 7.8$ provided that the temperature difference between two points of the finite element should not exceed 1, 2 and 3 units, and their ratio is 1.1. Using dependence (27) or (30) will result in the number of finite elements for the considered given accuracy values of calculations equal to 16, 8 and 5 elements, respectively.

To solve the system of linear equations, the Gaussian exclusion method or the square root method can be used, which provide good calculation accuracy with a small number of computational operations. Thermal characteristics are calculated based on the established nodal temperature values. The maximum temperature is defined as

$$T_{max} = max(T_1, T_2, \ldots, T_n)\ ; \quad (34)$$

where n is the number of nodes.

The average temperature $T_\varnothing$ is determined from the following equation:

$$T_\varnothing = \frac{\sum_{e=1}^{E} T_\varnothing^{(e)} L^{(e)}}{\sum_{e=1}^{E} L^{(e)}}\ ; \quad (35)$$

where $T_\varnothing^{(e)}$ is the average temperature of the finite element.

For example, according to the initial data, the number of finite elements of partition was determined by equation (32) and $E = 1.5$ and $\varepsilon = 1.1$ was obtained with $N_q = 10$.

The number of required temperature measurement points is determined by the degree of approximation of the approximating function to the dependence between temperature and displacement obtained in the experiment. The degree of approximation can be expressed by a measure of certainty (square of the regression coefficient). A certainty measure equal to one means complete coincidence and at the same time ideal approximation of the mathematical record of the task condition by the target function.

3.4 Evaluation of methods

Then, given the certainty measure, a suitable compensation function can be found for the selected areas of temperature measurement as part of the overall approximation function. In this way, the FEM can only help determine the number of temperature measurements, but does not answer the question of their minimum number and location. However, FEM determines the total number of finite elements over the entire length. . It is known that when steels and cast iron used in machine tools are heated by 1K (change in average temperature), there is a change in the length of 1 m by 11 μm. In accordance with (2), the minimum number of heat -active elements of the machine is one, and the maximum is six. Therefore, the resulting error is proportional to the number of such heated elements, parts, and assemblies. The model error in determining temperature deformations is calculated as follows:

$$\Delta = \frac{T_\varnothing - T_u}{T_\varnothing}\ ; \quad (36)$$

Then, the error will tend to zero if $T_u \to T_\varnothing$. As shown, this is possible only if the sensors are placed at points where the average temperatures are equal to the element temperature, and the probability of such placement is determined by the ratio of this range to the total length of the element. In other words, intuitively, the sensors are placed in places of the highest temperature. Therefore, as shown in Fig. 1 and 2, there is an error obtained determined by (36), which lies in the range from 12 to 40%. In addition, the random component of errors in the heat exchange conditions is not considered here, which will also lead to additional errors in the correction systems, which are also minimized by reducing the number and placement of temperature sensors.

4 SUMMARY

To solve the problems described above, thermal error compensation is provided for models without temperature sensors or with a minimum and reasonable number and location of their installation. This method has the following advantages: cost effectiveness, since no redundant data acquisition devices or sensors are required; reduced complexity of the control system since there is no need for online real-time temperature monitoring; eliminated errors caused by sensor instability and external factors. Therefore, the proposed method allows controlling the accuracy of TCP correction and determines the type, structure, parameters and characteristics of the system for controlling this correction process based on correlation, regression and other models.

5 REFERENCES

[Yto 2010] Yto Y.: Thermal deformation in Machine tools. McGraw-Hill, 2010, 214p

[Großmann 2015] Großmann K.: Thermo-energetic Design of Machine Tools. Springer, Switzerland, 2015, 261 p.

[Mayr 2012] Mayr J., Jedrzejewski J.: Thermal issues in machine tools CIRP Annals - Manufacturing Technology, (61) 2012, pp. 771–791.

[Ramesh 2000] Ramesh R., Mannan M.A.: Error compensation in machine tools — a review Part II: thermal errors. International Journal of Machine Tools & Manufacture (40) 2000. p.1257–1284

[Kuznetsov 2015] Kuznetsov A.P.: Probability Methods of Evaluation and Control of Precision Reliability of Metal-Cutting Machine Tools under Thermal Effects. Journal of Machinery Manufacture and Reliability, 2015, (44) /4, pp. 363–371.

[Kuznetsov 2018] Kuznetsov A.P., Koriath H.-J.: The methods for controlled thermal deformations in machine tools; 1st ICTIMT, Dresden, 2018, p. 47-60

[Kuznetsov 2019] Kuznetsov A. P.: Thermal processes in machine tools. - M.: Technosphere, 2019, 488p.

[Abdulshahed 2015] Abdulshahed Ali M. and Longstaff A.P.: The application of ANFIS prediction models for thermal error compensation on CNC machine tools. Applied Soft Computing 27 (2015) 158–168.

[Naumann 2018] Naumann C., et al.: Hybrid Correction of Thermal Errors using Temperature and Deformation Sensors. 1st ICTIMT Dresden, 2018.

[Xian 2018] Xian W.: Thermal Errors Classification Compensation without Sensor for CNC Machine Tools. Hindawi Mathematical Problems in Engineering Volume 2018, 11 pages.

[Hui 2020] Hui L.: Thermal error modeling for machine tools: Mechanistic analysis and solution for the pseudo correlation of temperature-sensitive points. IEEE

[Blaser 2019] Blaser P., Mayr J.: Long-Term Thermal Compensation of 5-Axis Machine Tools Due To Thermal Adaptive Learning Control. 15th International Conference on HSM 2019. MM Science Journal, 2019.